

Ionospheric Research
NASA Grant No. NGR-39-009-32

Scientific Report

on

"Evaluation of the Constant Momentum Mass
Spectrometer for Ionospheric Investigations"

by

H. M. Luther

November 1, 1966

Scientific Report No. 283

Ionosphere Research Laboratory

Submitted by:

B R F Kendall

B. R. F. Kendall, Associate Professor
of Physics, Project Supervisor

Approved by:

A. H. Waynick

A. H. Waynick, Director, Ionosphere
Research Laboratory

The Pennsylvania State University
College of Engineering
Department of Electrical Engineering

TABLE OF CONTENTS

	Page
Abstract	i
I. INTRODUCTION	
Basic Operating Principle	1
Amplification of the Initial Energy Distribution.	3
Resolving Power	4
A Mode of Operation Insensitive to the Initial Ion Energy Scatter	7
II. THE EXPERIMENTAL ANALYSIS	
Sequence of Experiments	8
Preliminary Studies	9
The First Mode of Operation	17
The Second Mode of Operation	20
The Third Mode of Operation	25
III. CONCLUSION	
Summary	29
BIBLIOGRAPHY.	32

ABSTRACT

A mass spectrometer is being developed in which pulsed fields give all ions the same momentum. The final ion energy is therefore mass dependent. A mass spectrum can be obtained by analyzing the energy distribution of the ions reaching the collector. The advantages of this type of spectrometer are compactness, simplicity, light weight, absence of magnets, and ability to operate at comparatively high pressures. These characteristics make the apparatus suitable for analyzing the ion composition of the lower regions of the ionosphere. Preliminary results of attempts to find operating conditions insensitive to initial ion energies are discussed.

I. INTRODUCTION

Basic Operating Principle

The constant momentum mass analyzer was originally proposed by J. A. Hipple.¹ A later paper by Fiks² proposed the same device, but neither author reported any experimental work on the analyzer. The first successfully operating constant momentum mass analyzer was described by Bracher.³

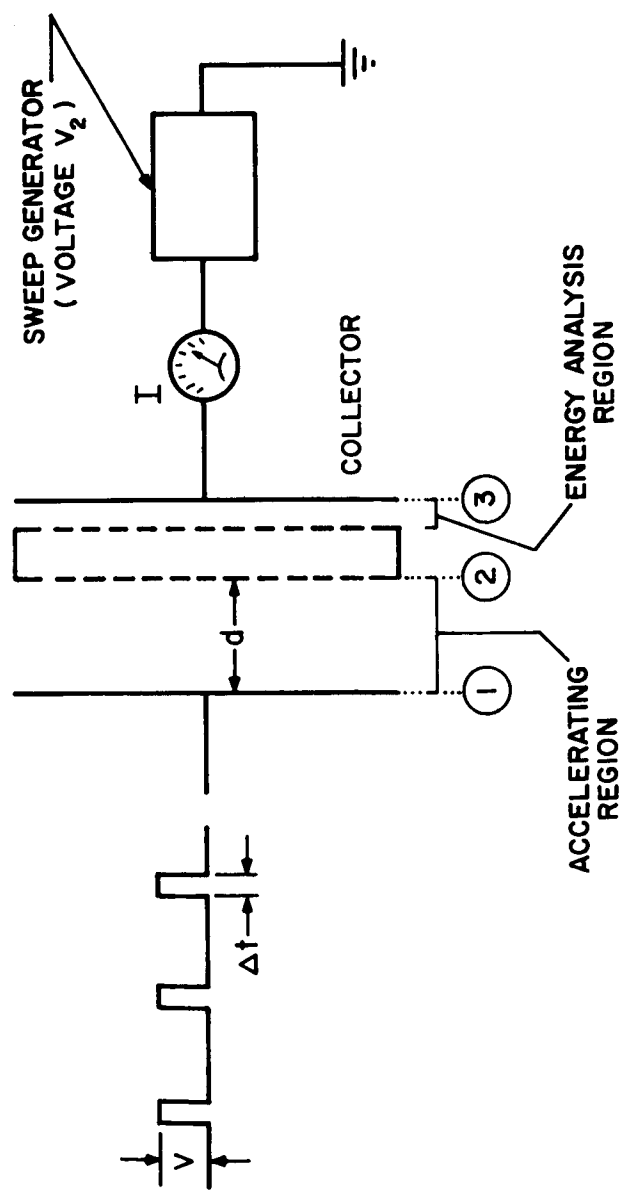
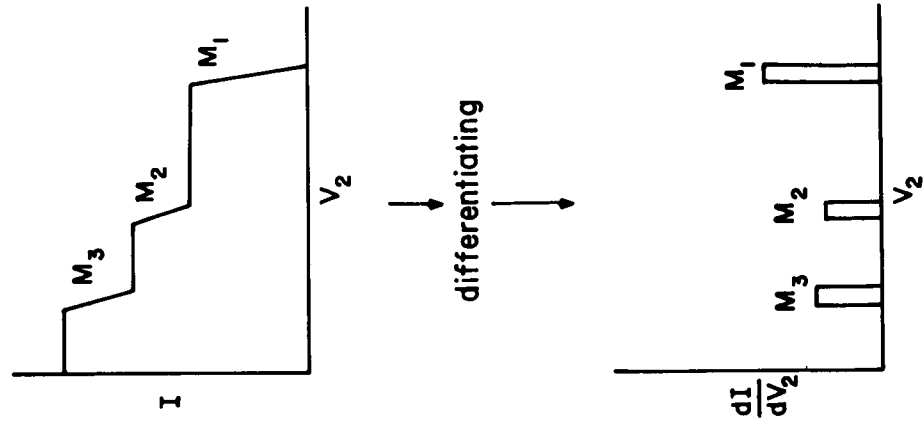
The basic operating principle of the constant momentum mass analyzer is shown in Figure 1. Ions are admitted into the region between electrodes (1) and (2) which are separated by a distance d , and then pulses of amplitude V and duration Δt are applied to electrode (1). The time Δt is chosen such that the ions to be analyzed do not have time to leave the region between the electrodes before the pulse is over. Under these conditions, all the ions, assuming them to be singly charged, gain the same momentum

$$\begin{aligned} P_c &= e \int E dt \\ &= \frac{e V \Delta t}{d} \end{aligned} \quad (1)$$

and thus the final ion energy will be

$$E = \frac{P_c^2}{2m} \quad (2)$$

I: ION CURRENT



BASIC CONSTANT - MOMENTUM MASS ANALYZER

FIGURE 1

so that

$$E = \frac{k}{m} \left(\frac{V \Delta t}{d} \right)^2 \quad (3)$$

where E is measured in electron volts, m in a.m.u., V in volts, Δt in μ secs. and d in cm, and k is a constant equal to 0.483.

The energy gain is therefore mass dependent and can be analyzed by sweeping a retarding field placed in front of an ion collector.

The advantages of such an analyzer include simplicity of operation and compactness. The analyzer can operate at pressures well above 10^{-3} Torr, since the dimensions of the spectrometer can be made less than the mean free path of the ions at such pressures. The instrument is therefore well-suited for positive ion analysis in the region of the ionosphere between 80 and 250 km where the pressure varies from 10^{-3} Torr to 10^{-7} Torr.

Amplification of the Initial Energy Distribution

A disadvantage of this type of analyzer is the limitation of resolving power by the initial energy distribution of the ions. This distribution is further amplified in the pulsing region. In order to obtain a quantitative estimate of this amplification, assume that the source ions have an initial energy distribution E_i about zero. The ions are all accelerated impulsively; hence, the final ion energy will be according to equation (3)

$$E_c = \frac{k C^2}{m} \quad (4)$$

with $C = \frac{V \Delta t}{d}$

and a distribution ΔE_f about E_c given by

$$\Delta E_f = \frac{1}{2m} [(\sqrt{2kC} + p_i)^2 - 2kC^2] \quad (5)$$

where $p_i = \sqrt{2m E_i}$. Thus ΔE_f is found to be

$$\Delta E_f = E_i + 2\sqrt{E_c E_i} \quad (6)$$

Since $\Delta E_f - E_i$ is larger than zero, E_i is amplified in Hipple's mass analyzer.

Resolving Power

Two definitions of resolving power are currently in use. The resolving power at a mass M is defined to be

$$R_M = \frac{M}{\Delta M} \quad (\text{definition 1})$$

where ΔM is the width of the mass peak in mass units. The resolving power may also be defined as that mass at which an adjacent peak can just be resolved. This definition is a special case of definition 1 and is obtained by requiring ΔM to be equal to 1 a.m.u.; then R_o is equal to the numerical value of the mass M_o

$$R_o = |M_o|. \quad (\text{definition 2})$$

Consider a beam of ions having mass M and $M + \Delta M$ and no initial energy distribution, i. e., $E_i = 0$. After the ions have been accelerated impulsively, the magnitude of the difference in the final ion energy will be, to first order in $\frac{\Delta M}{M}$ from equation (4),

$$\Delta E_c (M) = E_c (M) \frac{\Delta M}{M} \quad (7)$$

where $E_c (M) = \frac{k C^2}{M}$.

If the instrument can detect an energy ΔE_{\min} , then with $\Delta M = 1$ a. m. u. there will be a mass M_o such that

$$\Delta E_{\min} = \Delta E_c (M_o) = \left(\frac{1}{M_o} \right) E_c (M_o); \quad (8)$$

substituting equation (4) into equation (8) and letting $C = \frac{V \Delta t}{d}$, one obtains

$$R_o = | M_o | = \sqrt{\frac{E_c (1)}{\Delta E_{\min}}}, \quad (9)$$

where $E_c (1)$ is the impulsive energy gained by a proton.

Consider now a beam of ions of mass M with an initial energy scatter E_i . The resolving power of the mass analyzer at mass M will be according to definition (1) and using equation (7)

$$R_M = \frac{E_c (M)}{\Delta E_{\text{tot}} (M)}, \quad (10)$$

where $\Delta E_{\text{tot}} (M) = \Delta E_{\min} + 2 \Delta E_f (M)$. $\Delta E_f (M)$ has to be doubled if one assumes that the ions have a symmetric velocity distribution along the axis of the analyzer. Thus, combining

equations (6), (7) and (10)

$$R_M = \frac{E_c (M)}{\Delta E_{\min} + 2 E_i + 4 \sqrt{E_i E_c (M)}} \quad (11)$$

As $E_c (M)$ is made large

$$R_M \approx \frac{E_c (M)}{4 \sqrt{E_i E_c (M)}} \quad (12)$$

Finally, R_o is found from equation (12) to be

$$R_o = \left(\frac{1}{16} \frac{E_c (1)}{E_i} \right)^{1/3} \quad (13)$$

The dependence of R_o on $V^{2/3}$ is not quite in agreement with Bracher's³ presumably experimental result that

$$R_o \sim V^{1/2} \quad (14)$$

It is experimentally convenient to define the resolving power R_M of the spectrometer as

$$R_M = \left[\frac{E (M)}{\Delta E_{\text{tot}} (M)} \right]_{0.5} \quad (15)$$

where the subscript 0.5 indicates that the measurement is made at the half-height of the mass peak. Equations (12), (13) and (6) show that the constant momentum mass-analyzer is very sensitive

to the initial ion energy distribution. Successful operation of such an analyzer, therefore, demands some energy focusing either in the pulsing region or in the source.

A Mode of Operation Insensitive to the Initial Ion Energy Scatter

Consider an ion bunch entering the pulsing region with an initial energy E_i and a distribution ΔE_i about this energy. If now the ions are decelerated impulsively, the final ion energy will be

$$E_f = \frac{1}{2m} [p_i - \sqrt{2kC}]^2 \quad (16)$$

with a perturbation of ΔE_f about E_f given by

$$\Delta E_f = \frac{1}{2m} [(p_i + \Delta p_i - \sqrt{2kC})^2 - (p_i - \sqrt{2kC})^2] \quad (17)$$

where $p_i = \sqrt{2mE_i}$ is the initial momentum given to the ions and Δp_i is the differential scatter about p_i . Thus, $\Delta p_i = \frac{1}{2} \sqrt{\frac{2m}{E_i}} \Delta E_i$. Expanding the equation (17), one obtains

$$\Delta E_f = \Delta E_i \left[1 - \sqrt{\frac{E_c}{E_i}} + \frac{1}{4} \frac{\Delta E_i}{E_i} \right] \quad (18)$$

where $E_c = \frac{k C^2}{m}$. Neglecting the last term, one obtains

$$\Delta E_f \approx \Delta E_i \left(1 - \sqrt{\frac{E_c}{E_i}} \right) \quad (19)$$

The factor $1 - \sqrt{\frac{E_c}{E_i}}$ will be less than unity, and approaches zero as E_c approaches E_i . An impulsive retarding field placed in front of an ion collector would thus stop those ions for which E_c (M) is equal to the initial energy E_i . A mass spectrum can be obtained by sweeping this impulsive retarding field and then differentiating the collector current with respect to the ion energy. This mode of operation would retain all the advantages of the mass analyzer proposed by Hipple and would further be insensitive to the initial ion energy distribution.

II. THE EXPERIMENTAL ANALYSES

Sequence of Experiments

Three modes of operation of the constant momentum mass analyzer were studied experimentally. In the first two the ions are accelerated, whereas in the third mode of operation the ions are decelerated. The first mode of operation incorporates the basic mass analyzer only. An ion bunching field has been added to provide a measure of ion energy focusing in the second mode of operation.

Finally, the third mode of operation tests the implications of equation (19).

Preliminary Studies

The experimental apparatus involved in these investigations consisted of a frame into which could be mounted ion sources, collectors, and grids. This frame, entirely analogous to the familiar optical bench, has been described in detail in an article published in the American Journal of Physics.⁴ Using procedures outlined in that paper a K^+ ion surface ionization source was constructed. This source is shown in Figure 2H. A tungsten button 0.3 cm. in diameter was spot welded onto the filament to provide an equipotential surface from which the ions were emitted. A grid close to the surface created the necessary field gradient at the emitting surface. The filament of the ion source was heated with an alternating current. A potentiometer connected across the filament and into a d.c. power supply kept the emitting region of the filament at a definite time-invariant potential relative to the collector. Initial tests attempted to identify those parameters affecting the measured energy distribution of the ions in the beam. Figure (3) shows the essential details of the testing procedure. K^+ ions having an initial energy E_i are incident on the analyzing electrode (1) to which is applied a ramp function voltage as shown below that grid. The same voltage is also applied to the X axis of the X - Y recorder. The col-

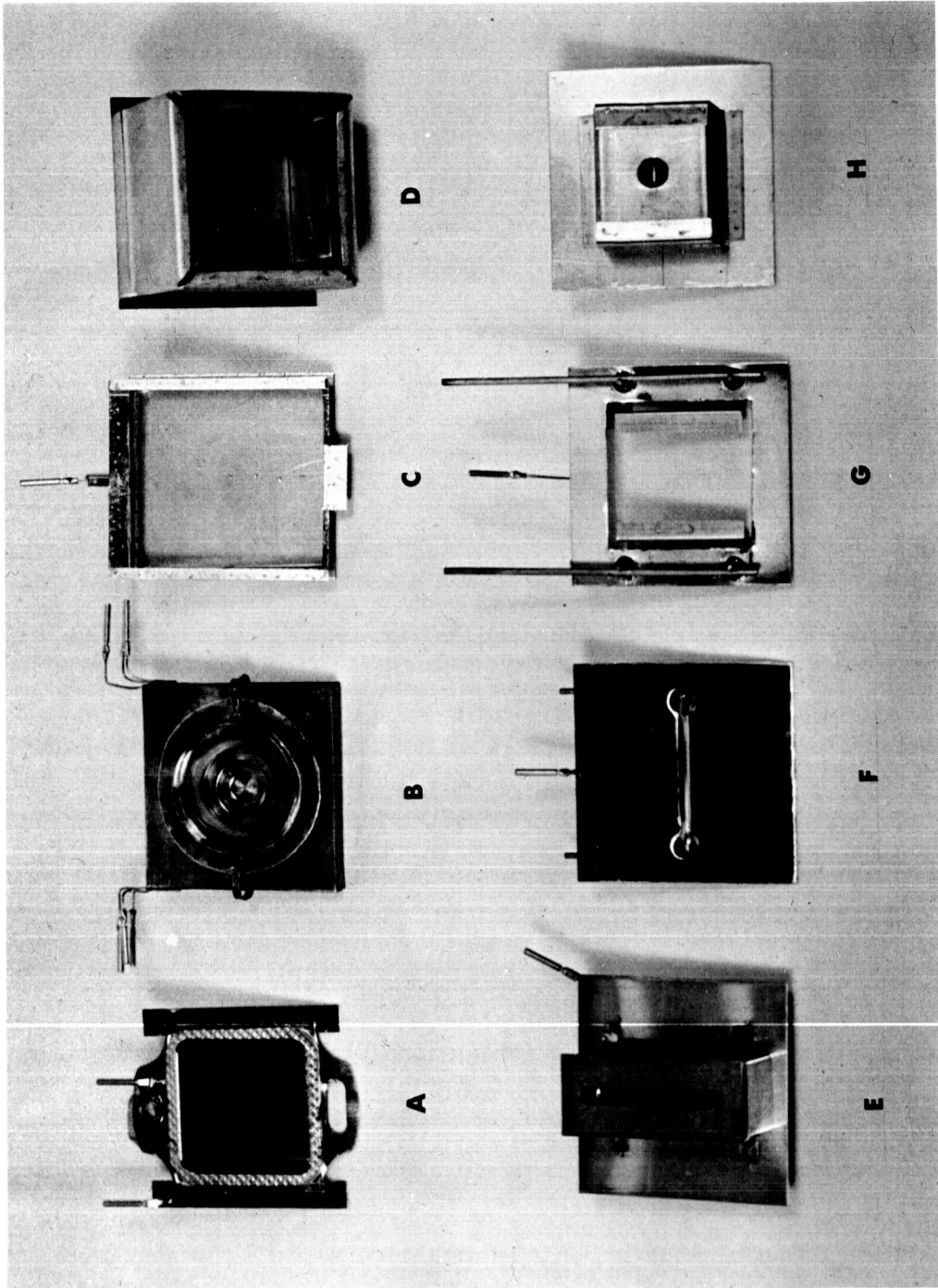
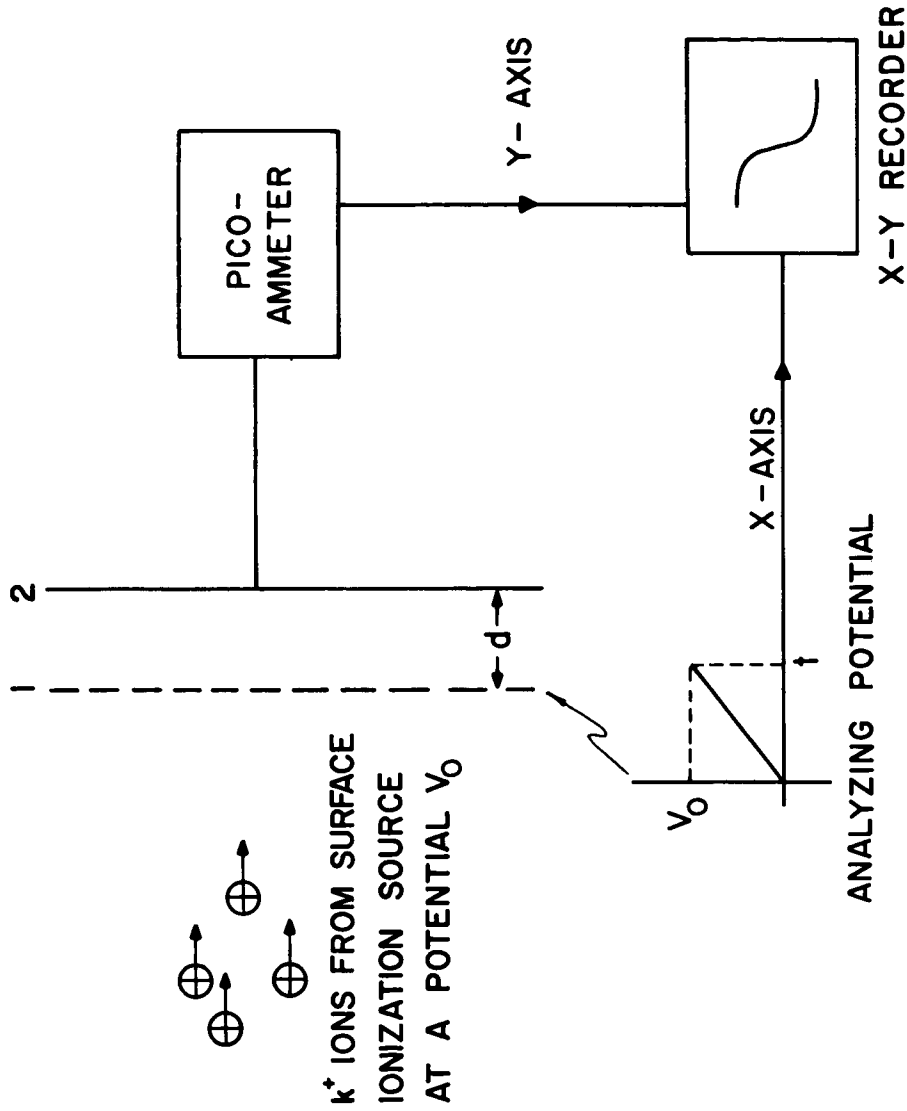


Fig. 2 Examples of Collectors (A-D) and Emitters (E-H).

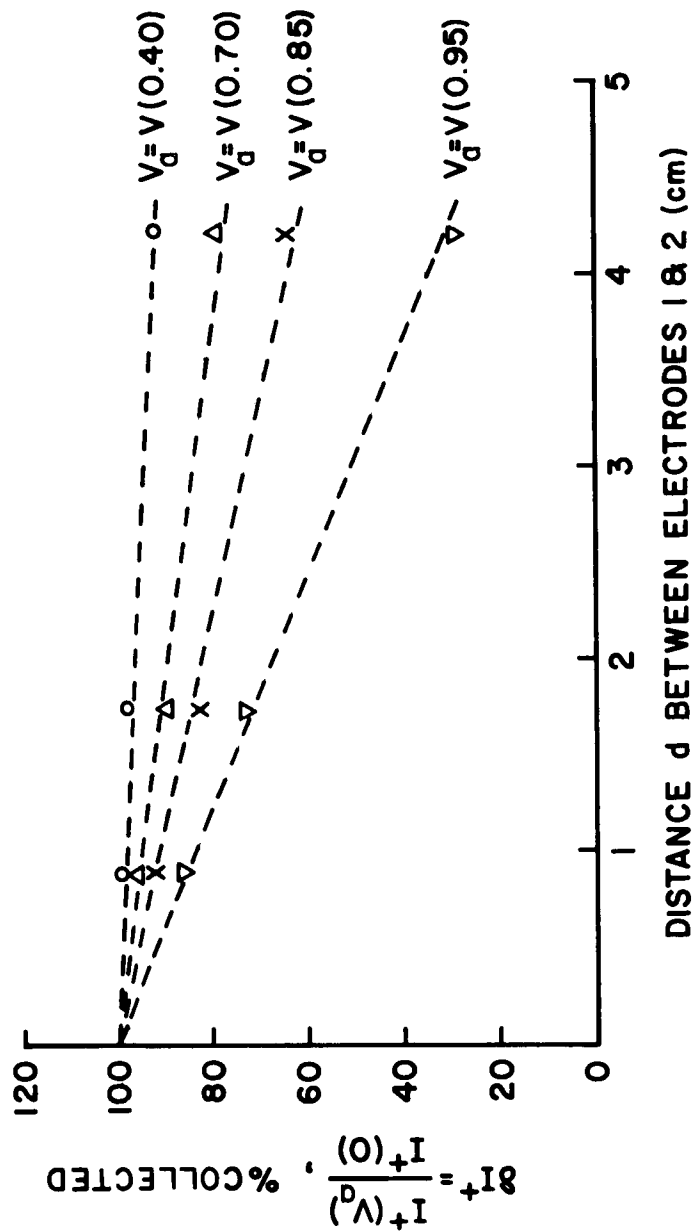


BLOCK DIAGRAM OF APPARATUS USED TO MEASURE ION ENERGY
FIGURE 3

lector is the electrode (2). This electrode initially was just a flat piece of stainless steel. The output of the picoammeter was then recorded on the Y axis of the X-Y recorder as a function of the analyzing voltage. It was found that the measured ion energy distribution was very sensitive to voltage fluctuations at the emitting surface, the distribution of a sample material on the emitting surface, and the procedure for ion energy analysis. Voltage fluctuations at the emitting surface could be applied by changing the potentiometer across the filament, i. e. moving the point of definite time-invariant potential away from the button. The fluctuations increased the energy distribution towards the higher energies. Since the emission efficiency of a surface ionization ion source increases monotonically with the field gradient across the surface, the observed change in the ion energy distribution is according to theory. The potentiometer was routinely adjusted so that a minimum energy distribution about the initial energy was obtained. The distribution of sample material on the tungsten button also affected the ion energy distribution. Excessive sample coverage increased the distribution towards lower energies. This observation can be explained by assuming that a number of ions are emitted from the surface of the fused sample material which would be at a lower potential than the tungsten surface. In order to eliminate this difficulty, a loading procedure was

developed which yielded reproducible energy distributions under identical conditions from sample to sample. The tungsten button was heated to cir. 180° C with infra-red lamps; then a drop of a solution containing the sample material KNO_3 was placed on the button. The water was flashed off leaving a fine dust of KNO_3 on the button.

The procedure for the analysis of the ion energies affected the measured energy distribution significantly, increasing the distribution towards the lower energies. Constant-energy tests were made using apparatus outlined in Figure 3. The results of these tests are shown in Figure 4 which is a graph of the relative change in the collected ion current as a function of the distance d for several values of the analyzing voltage. Figure 4 indicates that the analyzing electrode defocuses the ion beam. This interpretation is made plausible by considering the momentum of an ion in the beam. Since the ions are emitted into a solid angle from the source, some of them will have components of momentum transverse to the beam. This component is not affected by the analyzing field, and therefore, the ions will follow a curved trajectory which decreases the radial current density. If $J(r, l, V_a)$ is this density with r the radial distance from the axis of the beam, l the distance from the collector, and V_a the analyzing voltage, then



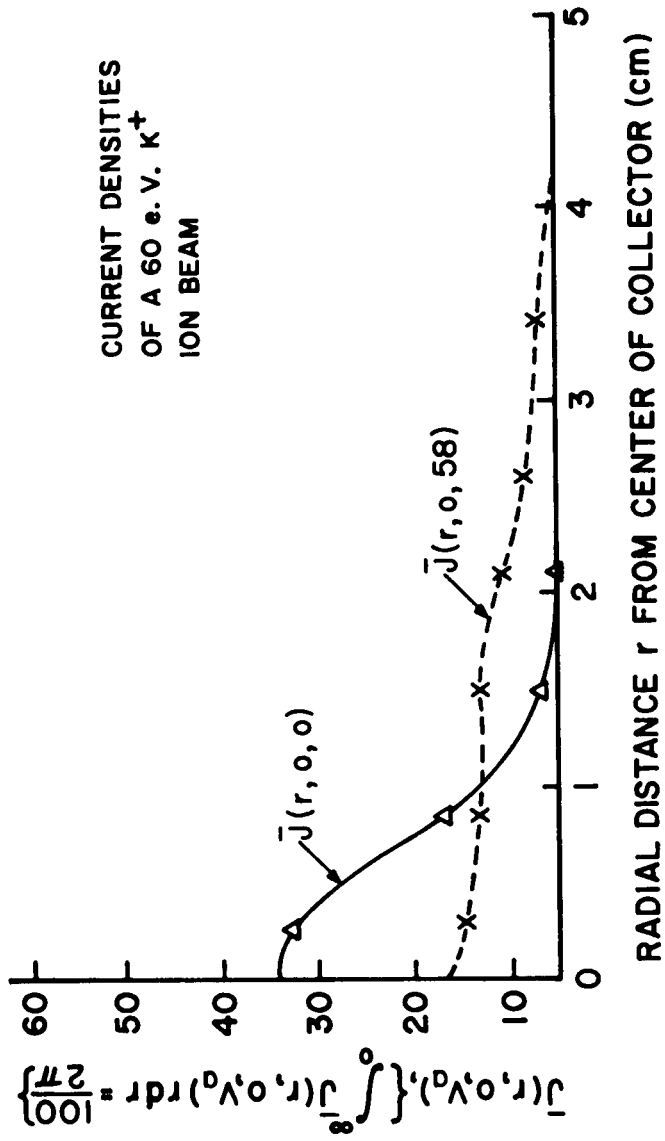
ION CURRENT LOSS vs ANALYZER-COLLECTOR DISTANCE

FIGURE 4

$$\delta I^+ = 1 - \frac{2\pi}{I^+(o)} \left\{ \int_{r_o}^{\infty} J(r, d, V_a) r dr + \int_{r_c}^{\infty} J(r, o, V_a) r dr \right\} \quad (19)$$

where r_o is the aperture radius of the analyzing electrode, $I^+(o)$ is the collector current with no retarding field, and r_c is the radius of the collector. δI^+ is the relative change in the collector current as a function of the parameters: d, V_a, r_o, r_c . The effect of the second integral has been studied, and it was found that this integral is much larger than the first. An annular collector was constructed of alternate layers of stainless steel plate and mica bonded together with a resin having a low vapour pressure.⁵ Figure 2B shows the completed assembly. Each ring was successively connected to a picoammeter to measure the ion current incident on that ring as a function of the analyzing voltage. The ion current incident on the i 'th ring divided by the area of that ring yielded an average current density $\bar{J}(r_i, O, V_a)$ where r_i is the mean radius of the i 'th ring. This quantity was then graphed as a function of r for different values of the parameter V . Some results are shown in Figure 5.

In order to determine an upper limit to the magnitude of the term $\int_{r_o}^{\infty} J(r, d, V_a) r dr$, a collector was constructed which collected all ions traversing the analyzing electrode. Such a collector is shown in Figure 2 D. A frame of mica was bonded onto the shield and a suppressor grid was attached to the mica.



CURRENT DENSITY vs ANALYZING VOLTAGE

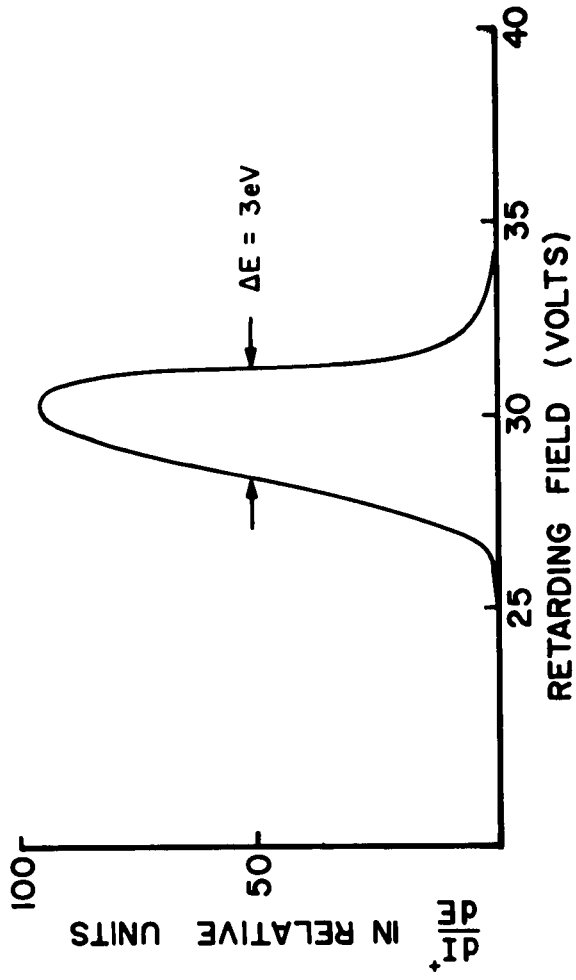
FIGURE 5

Tests using this collector geometry yielded results shown in Figure 6 which is the derivative of a plot of the picoammeter output as a function of the analyzing voltage. The total width of the energy distribution of the ions in the beam is about 3 eV and is nearly independent of the accelerating voltage. This distribution includes the apparent distribution caused by the defocusing effect of the ions in front of the analyzer and the real energy distribution of the ions. The ion energy spread was also affected by space charge effects which appeared when the ion current was larger than 10^{-8} amps. The effect of space charge was easily detectable from the increase of the ion current just before the accelerating voltage was reached by the analyzing field. Space charge effects vanished below 5×10^{-9} amps.

The three modes of operation described previously will now be discussed from the experimental view-point and results evaluated.

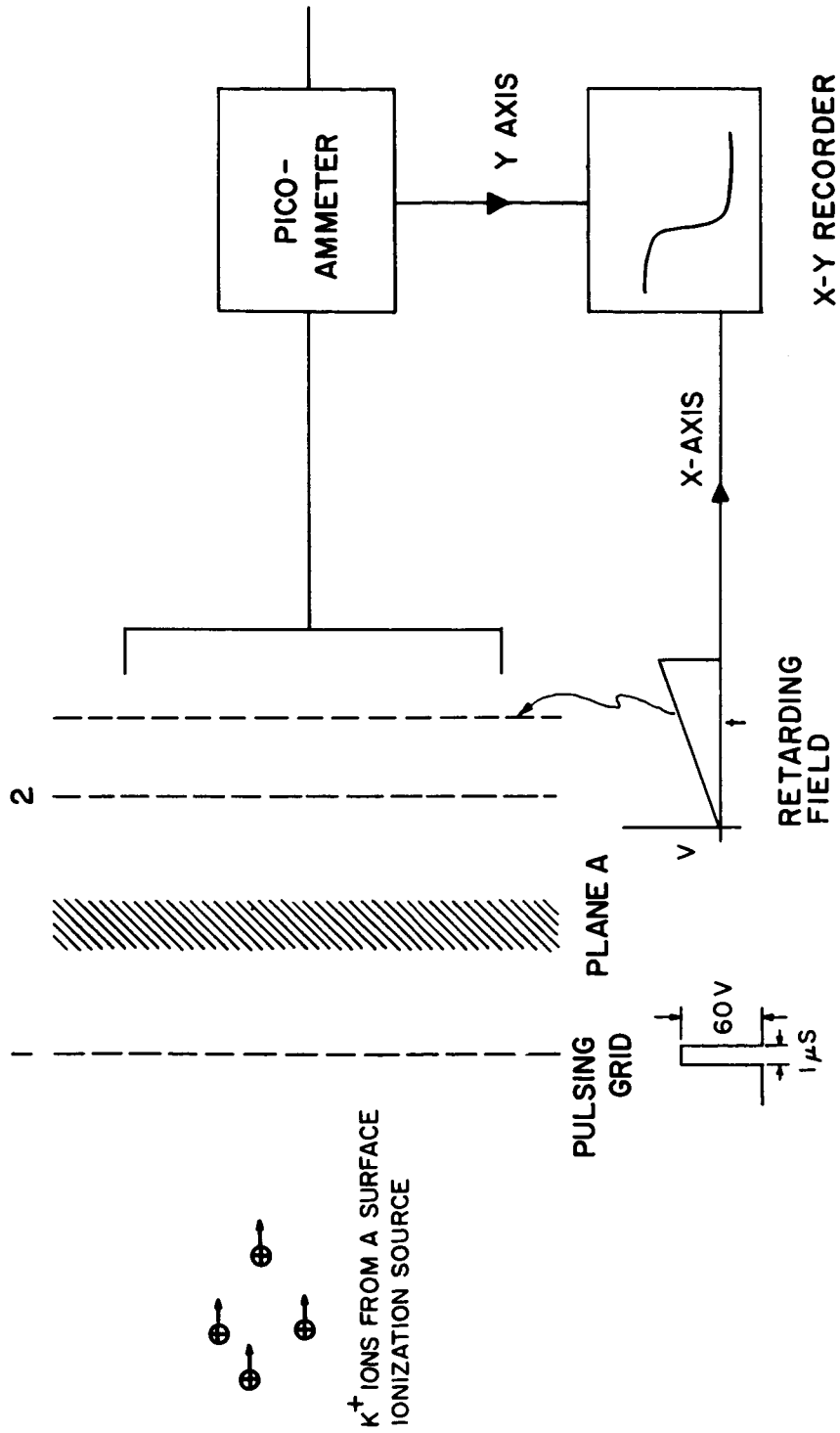
The First Mode of Operation

Having determined the most suitable analyzer-collector geometry, work using pulsed fields could proceed. In order to insure the most uniform analyzing field with adequate transmission, double grids of photo-etched nickel were used. The first mode, also the simplest, is shown in Figure 7. The ions are reflected



CONSTANT ENERGY TEST WITH DC FIELDS

FIGURE 6



ACCELERATING MODE I OF THE CONSTANT MOMENTUM MASS ANALYZER

FIGURE 7

in a plane A inside the pulsing region by a small d c bias voltage applied to the electrodes (1) and (2). A large positive pulse is applied to the electrode (1) and the final ion energies are analyzed with a sawtooth retarding field. The output of the picoammeter can be displayed as a function of the retarding voltage with an X-Y recorder. The mass spectrum can then be obtained by differentiating the output of the X-Y recorder. Since the ion energy varies as m^{-1} , the mass scale obtained will be in units of m^{-1} . The impulsive energy gained by the K^+ ions was typically about 25 eV, and the effective resolving power with an analyzing system about 1.25 cm. long was found to be

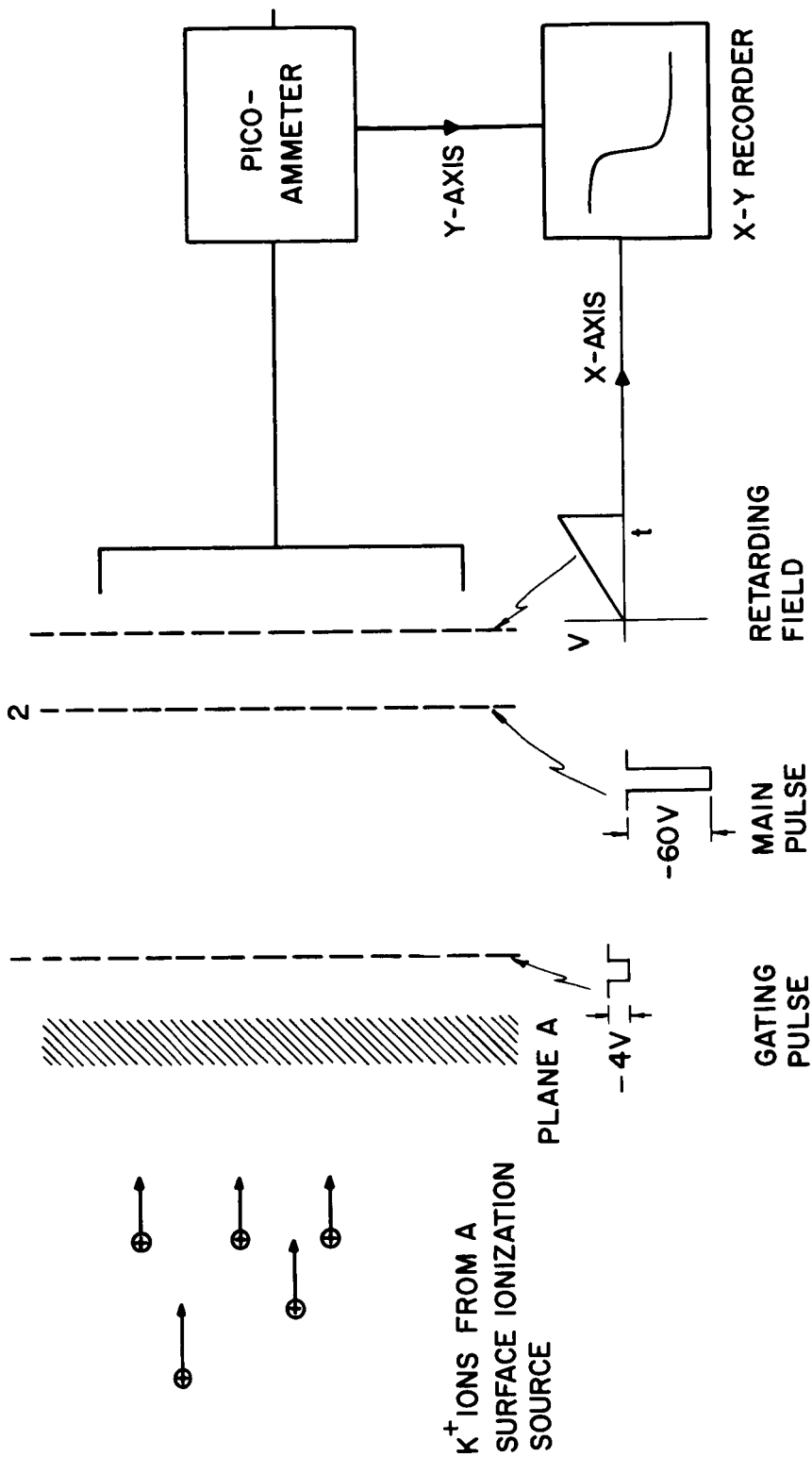
$$R_{K^+} = \left[\frac{E_c (K^+)}{5} \right]_{0.5} \approx 5$$

where the subscript 0.5 indicates that R_{K^+} was measured at half-height of the K^+ peak. This somewhat modest resolution is approximately what theory predicts for such a system.

The Second Mode of Operation

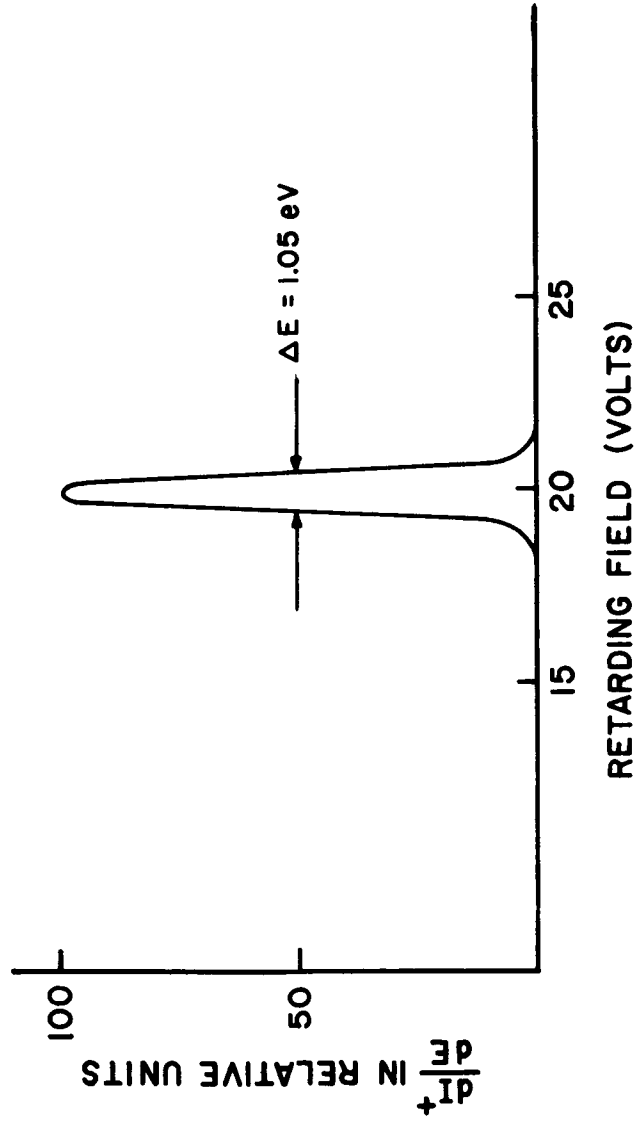
It is somewhat difficult to control the ion beam with d.c. bias voltages alone. In order, therefore, to control the ion beam more efficiently, a gate pulse was applied to the grid in front of the pulsing region, and the d c bias voltages were adjusted such that the

ions would reflect just in front of this grid. The details of this mode of operation are shown in Figure 8. The small negative pulse applied to grid (1) admits a cloud of ions into the pulsing region. The gate pulse triggers the main pulse applied to grid (2). A variable delay line between the gating pulse generator and the main pulsing unit insures that the ions are all inside the pulsing region before they are accelerated. As in the first mode, the ion energies are analyzed with a sawtooth retarding voltage. Constant-energy tests were made to determine the effect of the gate pulse upon the ion energies. Typical results are shown in Figure 9, which, like Figure 6, shows the derivative of the collector current with respect to the ion energy as a function of the analyzing voltage. The total width of the ion energy distribution at half height is approximately 1.05 eV. This distribution was found to be dependent upon the heights and duration of the gate pulse and the position of the reflecting plane A. The dependence of the ion energy distribution upon these parameters is to be expected, since the gate pulse actually controls the ion energy distribution of the ions entering the pulsing region, admitting only the more energetic ions from the source. The constant-energy test thus showed that one can decrease the ion energy distribution at the cost of decreasing the sensitivity of the mass analyzer. Tests with pulsed fields were subsequently made with the gate parameters optimized, and the results are shown in Figure 10. The 41_{K}^{+} and 39_{K}^{+} peaks have just

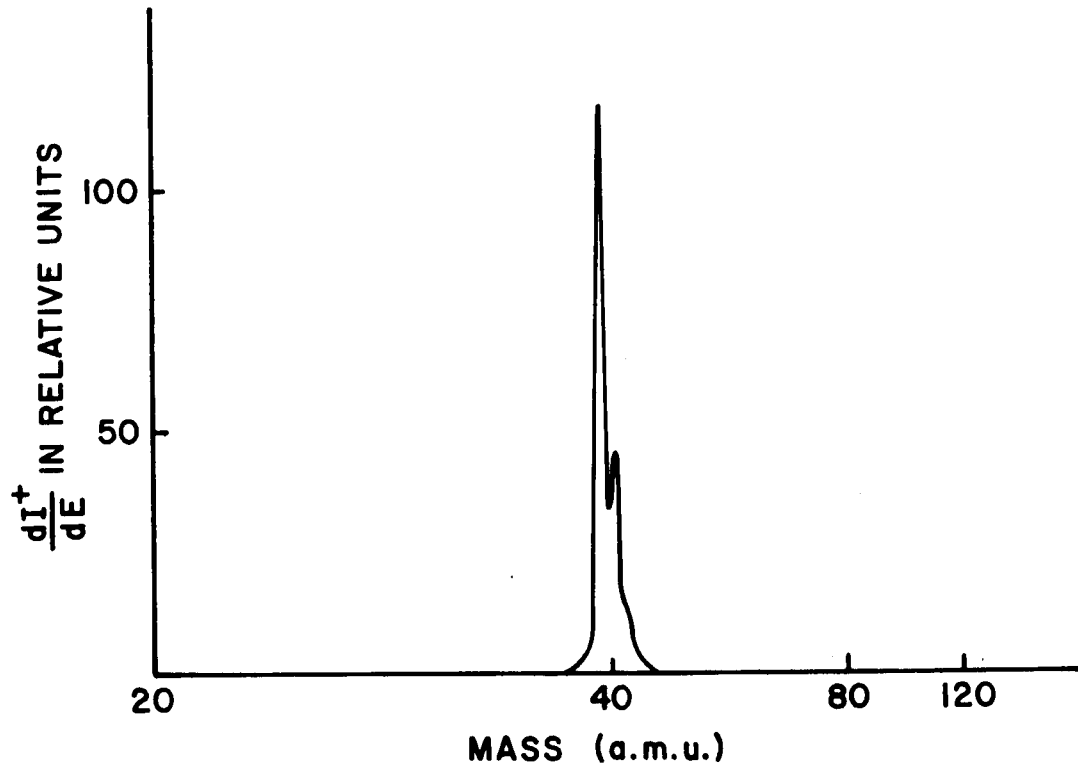


ACCELERATING MODE II OF THE CONSTANT MOMENTUM MASS ANALYZER

FIGURE 8



CONSTANT-ENERGY TEST WITH D.C. FIELDS & ION GATE
FIGURE 9

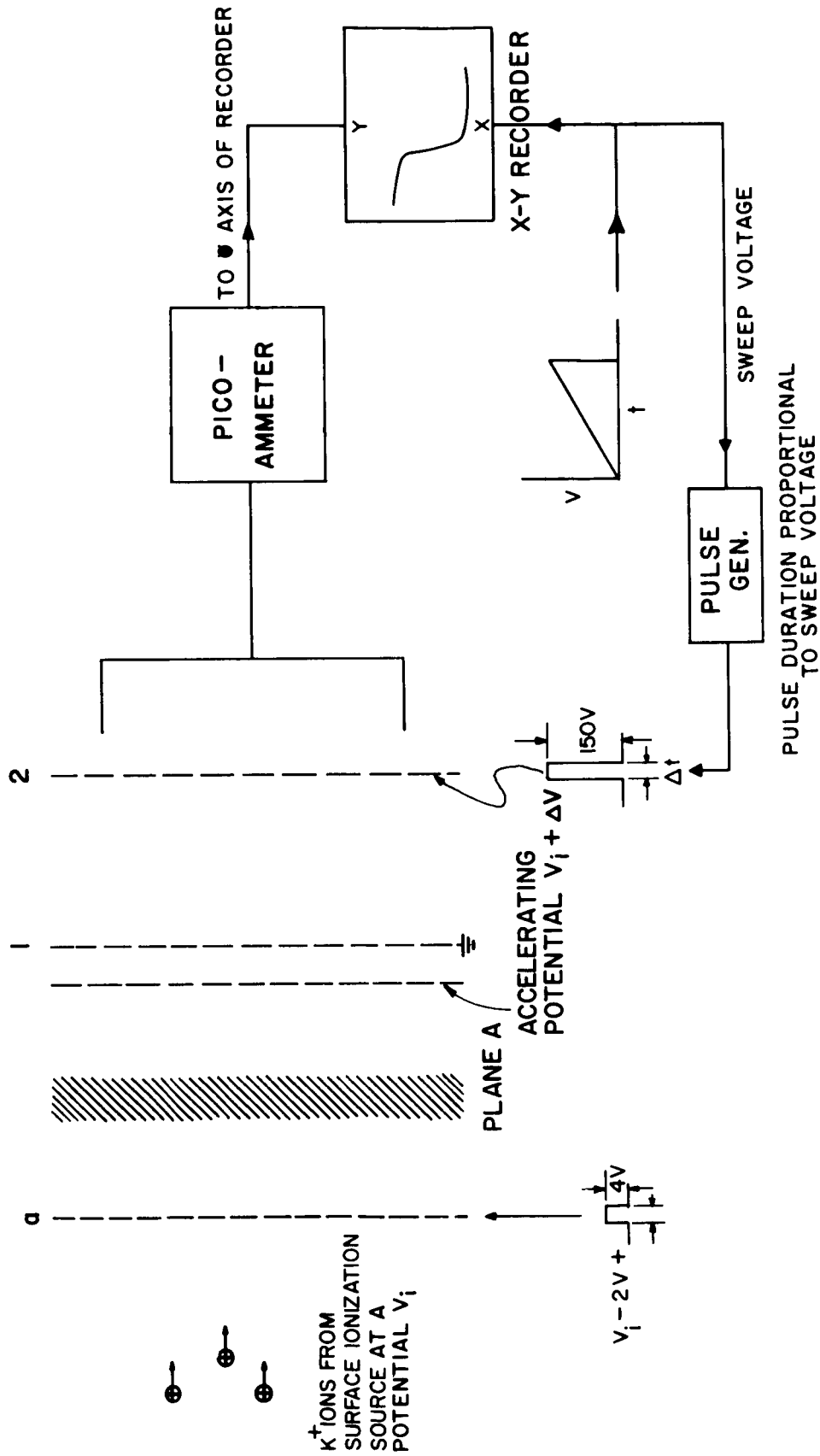


MASS SPECTRUM OF $^{39}\text{K}^+$, $^{41}\text{K}^+$
FROM SECOND OPERATING MODE
FIGURE 10

been resolved in this plot of the derivative of the collector current with respect to the ion energy. The peak ratio 41_{K}^{+} to 39_{K}^{+} is about 0.08 which is the natural ratio of abundances for potassium. The resolving power of the mass analyzer in this mode of operation is thus found to be about 20. There are two arguments against the 2nd mode of operation. The attractive features of the constant momentum mass analyzer are its high sensitivity and simplicity of operation. The gate that was used to resolve the potassium peak traded a favorable energy distribution against sensitivity. Further, the gate parameters were found to be very sensitive to the ion source condition and thus difficult to optimize for ions over a wide mass range. This operating mode, therefore, is both insensitive and imprecise.

The Third Mode of Operation

The third mode of operation investigated is based on equation (19). This mode should be most effective, since it was shown to be insensitive to the initial ion energy distribution. The essential details of this mass analyzer are shown in Figure 11. Ions from the K^{+} source at a voltage V_i are gated into the pulsing region between grids (1) and (2) with grid (a). These ions have a definite initial energy E_i . A positive pulse applied at grid (2) subtracts an impulsive energy from the initial energy of the ion; the ions are collected in a Faraday cage. The ion energies are analyzed by sweeping



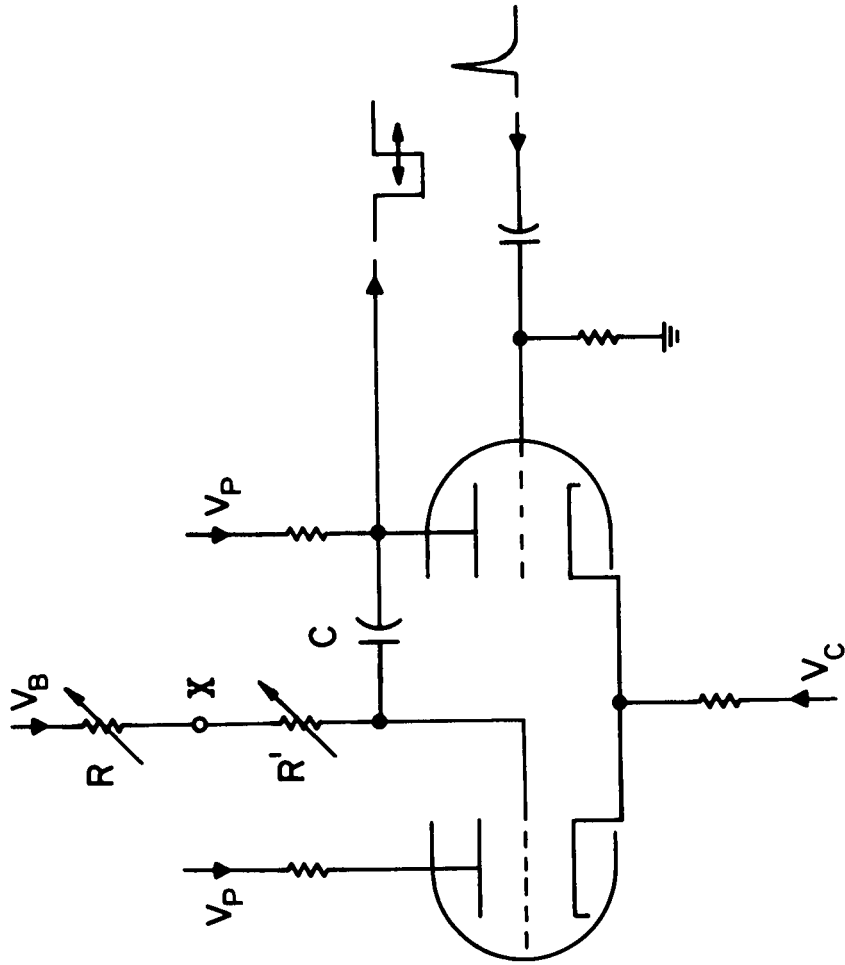
DECELERATING MODE OF THE CONSTANT MOMENTUM MASS ANALYZER

FIGURE 11

the pulse duration of the main pulse keeping the initial ion energy constant. The derivative of the output of the picoammeter with respect to the ion energy yields the mass spectrum. One advantage of this analyzer lies in the fact that a separate ion energy analyzing field is not needed. The complex ion energy analysis in this mode of operation required some modifications of the electronic apparatus.

In order to sweep the time duration of the pulse, a time varying voltage was applied to the grid circuit of the multivibrator controlling the pulse duration. The time-varying bias voltage can be obtained either mechanically by varying the resistor R in Figure 12 or electrically by disconnecting the circuit at the point marked x and then applying an external time-varying voltage. The latter method has the advantage that one can adjust the voltage $V(t)$ such that one obtains a convenient mass scale. In order to prevent loss of ions due to the defocusing action of the impulsive field, a collector which surrounded the pulsing region was constructed. A series of 3 evenly spaced grids connected to a pulse-voltage divider circuit insured that the impulsive field was spatially linear.

One objection to the ion gate used in the second mode was its excessive attenuation of the source ion beam. A new ion gate was therefore devised which would admit ion bunches into the pulsing region without attenuating the ion beam unduly. This gate is



PULSE-WIDTH MULTIVIBRATOR
FIGURE 12

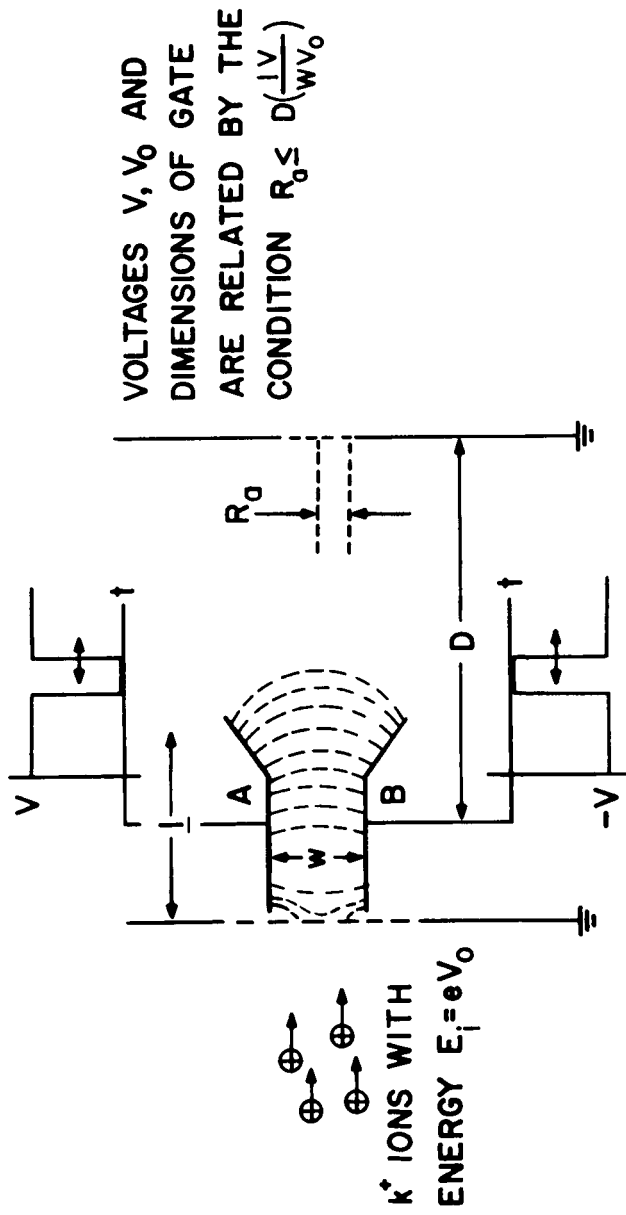
shown in Figure 13. The plates A and B are both bent in order to obtain a curved field on the exit side of the gate. It was found experimentally that the source ion beam was diminished by a factor approximately equal to the duty cycle of the gate pulse generator; further decreasing the pulse voltage decreased the ion energy distribution without attenuating the ion current significantly.

Initial experiments with the decelerating mode of operation yielded data comparable to the results obtained from the first accelerating mode of operation. Two facts were noted, however, the resolution, although low, increased with the pulse height of the decelerating pulse in the range from 50-100 volts and initial ion energies of cir. 40 eV. The resolution was very sensitive to the delay-time between the gate pulse and the decelerating pulse. The latter observation indicates that the length of the decelerating region was somewhat small for the pulse voltages available for decelerating the ions. Currently, a pulse amplifier is being constructed that will deliver 200 volt pulses.

III. CONCLUSION

Summary

The analyses of the three modes of operation have shown that the constant momentum mass analyzer can operate successfully provided some ion energy focusing method is added to the analyzer.



ION GATE FOR THIRD OPERATING MODE

FIGURE 13

Since the mass analyzer can be made very compact, it can be used at high pressures. Indeed, the second accelerating mode of operation has been tried at pressures around 10^{-4} Torr, and it was found that its performance did not deteriorate. The predicted high sensitivity of the of the mass analyzer has also been realized experimentally. Bracher obtained a sensitivity of 0.1 amp/Torr for neutral atoms.³ With operating voltages easily obtainable in airborne equipment a resolution of 20 was obtained, supporting the claim that a successful ion and neutrals analysis program of the lower E region can be carried out.

Bibliography

1. J. A. Hipple, U. S. Patent 2, 764, 691 (1956).
2. V. B. Fiks, Soviet Physics (Doklady), 1, 89, (1956).
3. J. Bracher, Zeit. Angew. Phys. 19, 347, (1965).
4. B. R. F. Kendall, H. M. Luther, Apparatus for Teaching and Research in Electron Physics, Am. Jour. Phys. 34, 580, (1966).
5. B. R. F. Kendall, M. F. Zabielski, Jour. Vac. Sci. Tech. 3, 114, (1966).